Chemistry–A European Journal
Research Article
doi.org/10.1002/chem.202104158
Chemistry Europe
European Chemical Societies Publishing
www.chemeurj.org

Bimodal Fluorescence/Magnetic Resonance Molecular Probes with Extended Spin Lifetimes

Shengjun Yang[+],[a, b] Philip Saul[+],[a, b] Salvatore Mamone,[a, b] Lukas Kaltschnee,[a, b] and Stefan Glöggler*[a, b]

Abstract: Bimodal molecular probes combining nuclear magnetic resonance (NMR) and fluorescence have been widely studied in basic science, as well as clinical research. The investigation of spin phenomena holds promise to broaden the scope of available probes allowing deeper insights into physiological processes. Herein, a class of molecules with a bimodal character with respect to fluorescence and nuclear spin singlet states is introduced. Singlet states are NMR silent but can be probed indirectly. Symmetric, perdeuterated molecules, in which the singlet states can be populated by vanishingly small electron-mediated couplings (below 1 Hz) are reported. The lifetimes of these states are an order of magnitude longer than the longitudinal relaxation times and up to four minutes at 7 T. Moreover, these molecules show either aggregation induced emission (AIE) or aggregation caused quenching (ACQ) with respect to their fluorescence. In the latter case, the existence of excited dimers, which are proposed to use in a switchable manner in combination with the quenching of nuclear spin singlet states, is observed

Multimodal molecular methods have been emerging as a powerful imaging tools in the scientific community as well as in the clinical practice.[1] Nuclear magnetic resonance (NMR) and fluorescence represent a particularly attractive combination for bimodal molecular probes because they can realize the complementary abilities of each modality – high spatial resolution with fluorescence and the detection of atomic-scale changes even in deep tissue via magnetic resonance – and therefore achieve greater effects.[2,3]

Phenomena related to extended nuclear spin order lifetimes by using long-lived nuclear singlet states (LLSS) are of interest for an emerging field of research aiming to discover novel molecular probes for magnetic resonance imaging.[4–13] Nuclear spin singlet states consist of two spin-1/2 nuclei coupling to a total spin 0 state.[4,14] This property endows the nuclear singlet state immunity to direct dipole-dipole interactions, a main contribution to longitudinal magnetization relaxation (T_1). Although the nuclear singlet state is NMR invisible and cannot be detected directly, Levitt and colleagues[15,16] revealed in 2004 that long-lived states can be probed. To date, several methods have been developed to populate the singlet spin order and evaluate the singlet equilibration time (T_S) between the singlet and triplet state.[4,15–23] The difference in chemical shift and *J*-couplings have been explored to populate singlet states, which was recently shown to be even possible via localized spectroscopy in vivo..[15–17,24–42] One prerequisite for a molecular system to support long-lived singlet lifetime is to incorporate an isolated spin-1/2 homonuclear pair in almost exact chemical equivalence. Chemically equivalent systems have the potential of supporting long-lived singlet lifetime because its symmetrical properties provide a protection against common relaxation mechanisms and thus do not allow for singlet-triplet leakage.[33,43] However, the chemically equivalent spin pair has no chemical shift difference and *J*-coupling difference is the only way allowing to populate singlet spin order since a transition between the two states requires a break in symmetry.[26,27] In such symmetric molecules, large (>5 Hz) *J*-coupling have mainly been investigated indicating close proximity of the additional spins to the singlet spin-pair. When using deuterons instead of protons, not only the *J*-couplings are significantly reduced but also dipolar effects in proximity to the singlet spin pair are significantly reduced. This is the main point here. Additionally to further remove dipolar effects, one would like to move all spins that do not form the singlet as far away as possible in the molecule. This will automatically lead to a reduction in *J*-coupling. Being able to access singlet states with very small *J*-couplings or perturbations of the symmetry hence means that we can work towards optimized singlet molecules with long-lifetime. In one example, a small *J*-coupling difference (<1 Hz) has been used to read-out long-lived spin order when the singlet spin order originated from *para*-hydrogen.[28,34] However the population of the singlet state in these cases was obtained by a reaction of a precursor with

[a] *Dr. S. Yang,[+] P. Saul,[+] S. Mamone, Dr. L. Kaltschnee, Dr. S. Glöggler*
Research Group for NMR Signal Enhancement
Max Planck Institute for Biophysical Chemistry
Am Fassberg 11, 37077 Göttingen (Germany)

[b] *Dr. S. Yang,[+] P. Saul,[+] S. Mamone, Dr. L. Kaltschnee, Dr. S. Glöggler*
Center for Biostructural Imaging of Neurodegeneration
Von-Siebold-Str.3 A, 37075 Göttingen (Germany)
E-mail: stefan.gloeggler@mpibpc.mpg.de

[+] *These authors contributed equally to the work.*

Supporting information for this article is available on the WWW under https://doi.org/10.1002/chem.202104158

para-hydrogen and subsequent transfer of the magnetization by means of field cycling[34] The particular long proton singlet states found in the latter studies underlines that an optimal design may be possible with minimized *J*-couplings in symmetric molecules. Therefore, it is of great interest to develop new molecular systems with long-lived singlet order created by the small *J*-coupling difference.

Herein, we introduce molecules that show fluorescent properties and display long-lived nuclear spin states. The latter are accessed via very small *J*-couplings (< 1 Hz) between ^{13}C or ^{15}N and ^{2}H spins to populate singlet states. The deuterium spins break the magnetic symmetry and significantly enhance the singlet lifetime compared to protonated counterparts. We have designed, synthesized and investigated perdeuterated $^{13}C_2$-TPE (tetraphenylethylene), DPP (diphenylphenanthrene) and DBC (dibenzochrysene) two of its derivatives, namely (figure 1a) and one fully deuterated ^{15}N-$^{15}N'$-diazobenzene compound (Figure 1b), which is a photo-switchable molecule with long LLSS in its protonated form.[44,45] The synthesis of the molecules is described in detail in the Supporting Information. The singlet states were investigated using the SLIC (spin-lock induced crossing) sequence with optimized spin-lock durations and nutation frequencies (Supporting Information).[46] The singlet decay curves for the TPE derivatives at $B_0 = 7$ T and for the azobenzene at $B_0 = 16.5$ T are depicted in figure 1c with all relaxation and singlet equilibration times reported in table 1. From the analysis of the signal build-up and 1D spectra, the ^{13}C-^{13}C *J*-coupling values of $^{13}C_2$-TPE-d_{20} and its derivatives were respectively determined as $^{1}J_{cc} = 71$ Hz, $^{3}J_{CD} = 0.82$ Hz and $^{4}J_{CD} < 0.1$ Hz for $^{13}C_2$-TPE-d_{20}, $^{1}J_{cc} = 62$ Hz, $^{3}J_{CD} = 1.55$ Hz and $^{4}J_{CD} < 0.1$ Hz for $^{13}C_2$-DPP-d_{18}, and $^{1}J_{cc} = 57$ Hz, $^{3}J_{CD} = 1.76$ Hz and $^{4}J_{CD} < 0.1$ Hz for $^{13}C_2$-DBC-d_{16}, whereby the ^{4}J coupling represents an estimate as this coupling could not be resolved.[26,27] These observations demonstrate that singlet spin order can still be populated by harnessing such small *J*-couplings.

Another chemically equivalent system with even smaller *J*-couplings that can be used to investigate singlet states is isotopically labeled ^{15}N,$^{15}N'$-azobenzene-d_{10}. The heteronuclear *J*-couplings found in the in trans-form were determined as $^{1}J_{NN} = 16$ Hz, $^{3}J_{ND} = 0.26$ Hz, $|^{4}J_{ND}| < 0.1$ Hz. Here, none of the nitrogen-deuterium couplings could be resolved and the couplings are estimated from the reported ^{15}N-^{1}H values, scaled by the difference in gyromagnetic ratio between protons and deuterium.[44,45] The T_1 value of $^{13}C_2$-TPE-d_{20} is about 22.7 s while the T_s of $^{13}C_2$-TPE-d_{20} dramatically increased to 243.5 s. The T_1 of $^{13}C_2$-DPP-d_{18} and $^{13}C_2$-TPE-d_{20} are similar and its T_s is slightly increased to 281.1 s. Unlike $^{13}C_2$-TPE-d_{20} and $^{13}C_2$-DPP-d_{18}, the T_1 and T_s value of $^{13}C_2$-DBC-d_{16} are significantly shortened to 15.2 s and 26.8 s. The determined T_s of the respective compounds illustrate, that, apart from chemical shift difference and *J*-couplings, the molecular symmetry plays a non-negligible role in the stability of the singlet state. Due to a steric hindrance DBC cannot maintain a planar form but is twisted. This effect contributes to the decrease in T_1 and T_s. The singlet lifetime of deuterated *trans*-^{15}N, $^{15}N'$-azobenzene-d_{10} is only 15.1 s, which is unexpectedly shorter than the protonated counterpart as reported by Ivanov et al.[44,45] We however note that in the deuterated molecule we observe a monoexponential decay only whereas in the reported protonated from, a much longer second exponential decay is observable. For comparison, we also synthesized the corresponding protonated molecules of the TPE derivatives and their T_1 and T_s value were also evaluated under the same conditions (Table 1). The T_1 value of $^{13}C_2$-TPE and $^{13}C_2$-DPP are comparable with their corresponding counterparts that is 16.1 s and 16.5 s, respectively. However, the T_s value of $^{13}C_2$-TPE and $^{13}C_2$-DPP shorten to 47.8 s and 40.6 s,

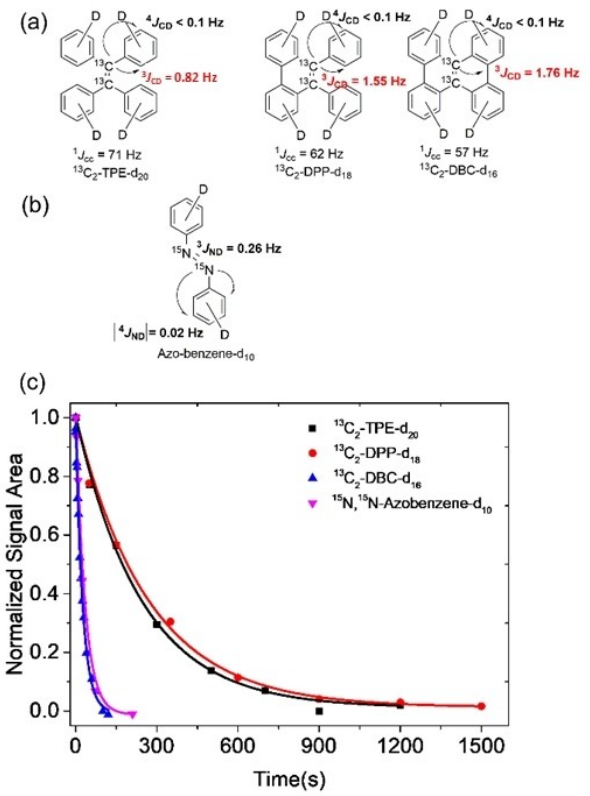

Figure 1. a) Molecular structure of fully deuterated $^{13}C_2$-TPE derivatives with *J* coupling values. b) The *J* couplings of *trans*-^{15}N, $^{15}N'$-azobenzene-d_{10}. c) Experimental decay curves of long-lived singlet state for $^{13}C_2$-TPE-d_{20}, $^{13}C_2$-DPP-d_{18}, $^{13}C_2$-DBC-d_{16} and *trans*-^{15}N,^{15}N-Azobenzene-d_{10}. All the samples were degassed by three times freeze-pump-thaw cycling. Experimental data points of fully deuterated $^{13}C_2$-TPE derivatives and *trans*-^{15}N, $^{15}N'$-azobenzene-d_{10} were observed at the magnetic fields of 7.05 T and 16.5 T, respectively. The pulse sequence SLIC[46] was employed and the data points have been normalized to the value of the first point. Solid lines are fitted to the exponential decays.

Table 1. Experimental value of T_1 and T_s of $^{13}C_2$-TPE-d_{20}, $^{13}C_2$-DPP-d_{18}, $^{13}C_2$-DBC-d_{16}, ^{15}N, $^{15}N'$-azobenzene-d_{10}, $^{13}C_2$-TPE, $^{13}C_2$-DPP and $^{13}C_2$-DBC.

Compounds	T_s (s)	T_1 (s)
$^{13}C_2$-TPE-d_{20}	243.5 ± 20.9	22.7 ± 0.1
$^{13}C_2$-DDP-d_{18}	281.1 ± 17.0	22.6 ± 0.1
$^{13}C_2$-DBC-d_{16}	26.8 ± 1.8	15.2 ± 0.0
^{15}N, ^{15}N-Azobenzene-d_{10}	15.2 ± 4.3	3.66 ± 0.1
$^{13}C_2$-TPE	47.8 ± 7.1	16.1 ± 0.1
$^{13}C_2$-DDP	40.6 ± 1.9	16.5 ± 0.2
$^{13}C_2$-DBC	20.3 ± 4.0	12.3 ± 0.3

All samples were degassed by three freeze-pump-thaw cycles.

respectively. $^{13}C_2$-DBC also has the similar tendency with its counterpart $^{13}C_2$-DBC-d_{16} that both of its T_1 and T_s shorten to 12.3 s and 20.3 s, respectively. The above results clearly show that the singlet state lifetime of $^{13}C_2$-TPE-d_{20} and $^{13}C_2$-DPP-d_{18} were extended more than 4-folds due to the deuteration and are still accessible via very small *J*-couplings adding another dimension to be considered when designing molecular probes with long lived singlet-states. These findings illustrate the impact of the *J*-coupling on the stability of the singlet-states and thus the significance of the deuteration of the compounds.

To get insight into the singlet lifetime changes between the deuterated ^{13}C molecules, their structure geometry were computed by the density functional theory (DFT) method B3LYP 6–31 + G(d, p). The optimized molecular geometry is shown in Figure 2, which are in accordance with the reported literatures.[47,48,49] From the results, $^{13}C_2$-TPE-d_{20} is a D_2 symmetrical molecule, while $^{13}C_2$-DPP-d_{18} is C_2 and $^{13}C_2$-DBC-d_{16} is D_2. Since the molecular geometry is significantly different, their optimized geometry parameters (Table s1) accordingly changed. The results showed that distances between the atoms, such as d (^{13}C-^{13}C), d (^{13}C, ^{2}H), d (^{2}H, ^{2}H) become shorter after the phenyl rings were locked. Thereafter, the chemical shift anisotropy CSA (^{13}C) also become larger after locking the rings.

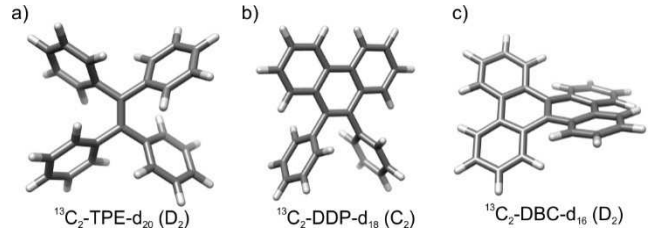

Figure 2. Structural models of $^{13}C_2$-TPE-d_{20} (a), $^{13}C_2$-DPP-d_{20} (b) and $^{13}C_2$-DBC-d_{20} (c) optimized at B3LYP 6–31 + G(d, p) density functional theory (DFT) level, using a polarizable continuum model for THF (for further information, see Supporting Information). The point groups resulting are given in parentheses.

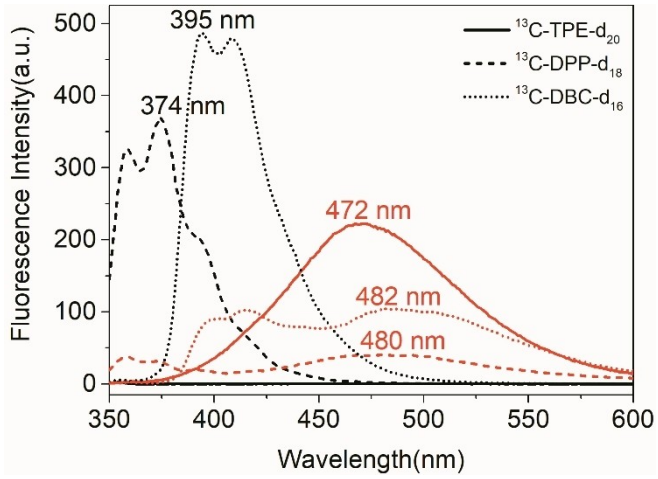

Figure 3. Fluorescence spectra of $^{13}C_2$-TPE-d_{20} (solid line), $^{13}C_2$-DPP-d_{18} (short dash line) and $^{13}C_2$-DBC-d_{16} (short dot line) at the concentration of 10 uM in THF-d_8 with the fraction of 0% (black) and 95% water (red).

Those results could draw a finding that the conformational change significantly affects the singlet state lifetime.

Fluorescence performance of $^{13}C_2$-TPE-d_{20}, $^{13}C_2$-DPP-d_{18} and $^{13}C_2$-DBC-d_{16} were subsequently investigated. As shown from fluorometry in Figure 3, $^{13}C_2$-TPE-d_{20} displays the same Aggregation Induced Emission (AIE) effect observed in protonated $^{13}C_2$-TPE.[31] The molecule of $^{13}C_2$-TPE-d_{20} is weakly fluorescent in the dissolved state in THF solution, while it switched to emit strong fluorescence centered at 472 nm in the presence of 95% water, where the aggregated state is formed.[50] In this aggregated state, TPE exhibits a fluorescence quantum yield of $\Phi_F = 0.13$.[51] The extinction coefficient has been determined to be $\varepsilon_{319} = 2550\ L \cdot mol^{-1}cm^{-1}$ leading to a brightness of $331\ L \cdot mol^{-1}cm^{-1}$, which is in the same order of magnitude of other fluorescence probes with AIE properties.[52,53] In sharp contrast, dissolved $^{13}C_2$-DPP-d_{18} emit strong fluorescence at the peak of 374 nm along with a shoulder at 358 nm, while the fluorescence intensity at the given wavelengths is quenched upon addition of 95% water. At a fluorescence quantum yield of $\Phi_F = 0.053$ in DPP[51] this leads to a brightness of $151\ L \cdot mol^{-1}cm^{-1}$ at an extinction coefficient of $\varepsilon_{307} = 2550\ L \cdot mol^{-1}cm^{-1}$. At the same time a red shifted band appears at 480 nm which can be attributed to excited dimers. Similarly, dissolved $^{13}C_2$-DBC-d_{16} emit strong fluorescence at the wavelength of 395 nm along with a shoulder at 408 nm, the fluorescence is quenched upon addition of 95% water and a new fluorescent peak emerges at the wavelength of 482 nm. In this case, for the non-aggregated compound, the extinction coefficient was determined to be $\varepsilon_{303} = 33700\ L \cdot mol^{-1}cm^{-1}$. $^{13}C_2$-DPP-d_{18}[51] and $^{13}C_2$-DBC-d_{16}[49] display an opposite phenomenon of AIE, which is termed aggregation-caused quenching (ACQ). The significant change in fluorescence behavior between $^{13}C_2$-TPE-d_{20} and $^{13}C_2$-DPP-d_{18}, $^{13}C_2$-DBC-d_{16} is related to their structural modification. Since the phenyl rings of $^{13}C_2$-DPP-d_{18}, $^{13}C_2$-DBC-d_{16} are covalently locked to form a conjugated structure, their intramolecular motion is restricted and therefore their fluorescence behavior is affected. For both the AIE or ACQ effect, a bimodal switching process is observed effecting the fluorescence and nuclear spins at the same time: Upon the aggregation the nuclear spin cannot be detected in the liquid anymore due to dipolar broadening of the lines, however the fluorescence serves as an indicative read-out. The change in fluorescence properties started at rather specific THF/H_2O ratios of 30:70 for $^{13}C_2$-TPE-d_{20}, and 20:80 for $^{13}C_2$-DPP and $^{13}C_2$-DBC-d_{16} respectively. In the same manner, the singlet state cannot be detected anymore at specific THF/D_2O ratios of 50:50 for $^{13}C_2$-TPE-d_{20}, 80:20 for $^{13}C_2$-DPP, and 65:35 for $^{13}C_2$-DBC-d_{16}.The spectra proving this behavior are displayed in the Supporting Information (page 7). This process is reversible once the solvent system is changed towards organic solvents and the water removed.

In conclusion, we have introduced a concept of 'on-off' switchable singlet NMR/fluorescence bimodal probe, whereby its singlet spin order can be accessed with small *J*-couplings (< 1 Hz). We have analyzed the influence of conformational changes on the singlet relaxation lifetime and we have demonstrated that singlet lifetimes up to 4 min are achievable at high fields. Moreover, addition of water significantly

quenches singlet lifetimes and effects their fluorescent properties. Although this has been mainly investigated here in an organic solvent system and the addition of water, tuning the molecules to for example sense ions in a biological context will be challenges for the future. In addition, the combination with techniques of magnetic resonance signal enhancement poses opportunities to develop the here proposed approaches into molecular probes for biomedicine.[54–58] Hence we envision the application potential as contrast agents or to map the biodistribution of photo-pharmaceuticals.[59]

Acknowledgements

We gratefully thank the Max-Planck-Society and the Max-Planck- Institute for Biophysical Chemistry for generous funding. This project has received funding from the European Research Council (ERC) under the European Union's Horizon 2020 research and innovation programme (Grant agreement No. 949180). Open Access funding enabled and organized by Projekt DEAL.

Conflict of Interest

The authors declare no conflict of interest.

Keywords: aggregation induced emission · aggregation caused quenching · bimodal contrast agents · fluorescence · NMR spectroscopy

[1] a) A. Louie, *Chem. Rev.* **2010**, *110*, 3146–3195; b) T.-H. Shin, Y. Choi, S. Kim, J. Cheon, *Chem. Soc. Rev.* **2015**, *44*, 4501–4516; c) L. E. Jennings, N. J. Long, *Chem. Commun.* **2009**, 3511–3524; d) T. Maldiney, B.-T. Doan, D. Alloyeau, M. Bessodes, D. Scherman, C. Richard, *Adv. Funct. Mater.* **2015**, *25*, 331–338; e) G. Angelovski, *Angew Chem. Int. Ed.* **2016**, *55*, 7038–7046.
[2] a) P. Verwilst, S. Park, B. Yoona, J. S. Kim, *Chem. Soc. Rev.* **2015**, *44*, 1791–1806; b) V. S. R. Harrison, C. E. Carney, K. W. Macrenaris, T. J. Meade, *Chem. Commun.* **2014**, *50*, 11469–11471; c) S. Yang, Y. Yuan, W. Jiang, L. Ren, H. Deng, L.-S. Bouchard, M. Liu, X. Zhou, *Chem. Eur. J.* **2017**, *23*, 7648–7652; d) V. S. R. Harrison, C. E. Carney, K. W. MacRenaris, E. A. Waters, T. J. Meade, *J. Am. Chem. Soc.* **2015**, *137*, 9108–9116.
[3] a) Z. Xu, C. Liu, S. Zhao, S. Chen, Y. Zhao, *Chem. Rev.* **2019**, *119*, 195–230; b) D. Xie, M. Yu, R. T. Kadakia, E. L. Que, *Acc. Chem. Res.* **2020**, *53*, 2–10.
[4] M. H. Levitt, *Annu. Rev. Phys. Chem.* **2012**, *63*, 89–105.
[5] Y. Feng, T. Theis, T.-L. Wu, K. Claytor, W. S. Warren, *J. Chem. Phys.* **2014**, *141*, 134307.
[6] M. C. D. Tayler, M. H. Levitt, *Phys. Chem. Chem. Phys.* **2011**, *13*, 9128–9130.
[7] P. Ahuja, R. Sarkar, P. R. Vasos, G. Bodenhausen, *J. Chem. Phys.* **2007**, *127*, 134112.
[8] M. H. Levitt, *J. Magn. Reson.* **2019**, *306*, 69–74.
[9] Y. Zhang, X. Duan, P. C. Soon, V. Sychrowsky, J. W. Canary, A. Jerschow, *ChemPhysChem* **2016**, *17*, 2967–2971.
[10] S. J. DeVience, R. Walsworth, M. S. Rosen, *NMR Biomed.* **2013**, *26*, 1204–1212.
[11] P. Nikolaou, B. M. Goodson, E. Y. Chekmenev, *Chem. Eur. J.* **2015**, *21*, 3156–3166.
[12] S. Glöggler, S. J. Elliott, G. Stevanato, R. C. D. Brown, M. H. Levitt, *RSC Adv.* **2017**, *55*, 34574–34578.
[13] S. Mamone, S. Glöggler, *Phys. Chem. Chem. Phys.* **2018**, *20*, 22463–22467.
[14] G. Pileio, *Prog. Nucl. Magn. Res. Spectr.* **2010**, *56*, 217–231.
[15] M. Carravetta, O. G. Johannessen, M. H. Levitt, *Phys. Rev. Lett.* **2004**, *92*, 153003.
[16] M. Carravetta, M. H. Levitt, *J. Am. Chem. Soc.* **2004**, *126*, 6228–6229.
[17] G. Pileio, M. Carravetta, M. H. Levitt, *Proc. Natl. Acad. Sci. USA* **2011**, *107*, 17135–17139.
[18] S. Mamone, N. Rezaei-Ghaleh, F. Opazo, C. Griesinger, S. Glöggler, *Sci. Adv.* **2020**, *6*, eaaz1955.
[19] R. Sarkar, P. R. Vasos, G. Bodenhausen, *J. Am. Chem. Soc.* **2007**, *129*, 328–334.
[20] A. S. Kiryutin, A. N. Pravditsev, A. V. Yurkovskaya, H.-M. Vieth, K. L. Ivanov, *J. Phys. Chem. B* **2016**, *120*, 11978–11986.
[21] A. N. Pravdivtsev, A. S. Kiryutin, A. V. Yurkovskaya, H. M. Vieth, K. L. Ivanov, *J. Magn. Reson.* **2016**, *273*, 56–64.
[22] B. Kharkov, X. Duan, E. S. Tovar, J. W. Canary, A. Jerschow, *Phys. Chem. Chem. Phys.* **2019**, *21*, 2595–2600.
[23] S. J. Elliott, G. Stevanato, *J. Magn. Reson.* **2019**, *301*, 49–55.
[24] M. C. D. Tayler, M. H. Levitt, *Phys. Chem. Chem. Phys.* **2011**, *13*, 5556–5560.
[25] G. Pileio, M. Carravetta, E. Hughes, M. H. Levitt, *J. Am. Chem. Soc.* **2008**, *130*, 12582–12583.
[26] Y. Feng, R. M. Davis, W. S. Warren, *Nat. Phys.* **2012**, *8*, 831–837.
[27] Y. Feng, T. Theis, X. Liang, Q. Wang, W. S. Warren, *J. Am. Chem. Soc.* **2013**, *135*, 9632–9635.
[28] M. B. Franzoni, L. Buljubasich, H. W. Spiess, K. Münnemann, *J. Am. Chem. Soc.* **2012**, *134*, 10393–10396.
[29] K. Claytor, T. Theis, Y. Feng, J. Yu, D. Gooden, W. S. Warren, *J. Am. Chem. Soc.* **2014**, *136*, 15118–15121.
[30] K. Claytor, T. Theis, Y. Feng, W. Warren, *J. Magn. Reson.* **2014**, *239*, 81–86.
[31] S. Yang, J. McCormick, S. Mamone, L.-S. Bouchard, S. Glöggler, *Angew. Chem. Int. Ed.* **2019**, *58*, 2879–2883.
[32] W. S. Warren, E. Jensita, R. T. Branca, X. Chen, *Science* **2009**, *323*, 1711–1714.
[33] G. Stevanato, J. T. Hill-Cousins, P. Håkansson, S. S. Roy, L. J. Brown, R. C. D. Brown, G. Pileio, M. H. Levitt, *Angew. Chem. Int. Ed.* **2015**, *54*, 3740–3743.
[34] Y. Zhang, P. C. Soon, A. Jerschow, J. W. Canary, *Angew. Chem. Int. Ed.* **2014**, *53*, 3396–3399.
[35] B. Procacci, S. S. Roy, P. Norcott, N. Turner, S. B. Duckett, *J. Am. Chem. Soc.* **2018**, *140*, 16855–16864.
[36] P. Saul, S. Mamone, S. Glöggler, *Chem. Sci.* **2019**, *10*, 413–417.
[37] M. Carravetta, M. H. Levitt, *J. Chem. Phys.* **2005**, *122*, 214505.
[38] G. Pileio, M. H. Levitt, *J. Chem. Phys.* **2009**, *130*, 214501.
[39] G. Pileio, S. Bowen, C. Laustsen, M. C. D. Tayler, J. T. Hill-Cousins, L. J. Brown, R. C. D. Brown, J. H. Ardenskjær-Larsen, M. H. Levitt, *J. Am. Chem. Soc.* **2013**, *135*, 5084–5088.
[40] T. Theis, G. X. Ortiz Jr, A. W. J. Logan, K. E. Claytor, Y. Feng, W. P. Huhn, V. Blum, S. J. Malcolmson, E. Y. Chekmenev, Q. Wang, W. S. Warren, *Sci. Adv.* **2016**, *2*, e1501438.
[41] C. Stavarache, A. Hanganu, A. Paun, C. Paraschivescu, M. Matache, P. R. Vasos, *J. Magn. Reson.* **2017**, *284*, 15–19.
[42] S. Mamone, A. B. Schmidt, N. Schwaderlapp, T. Lange, D. v. Elverfeldt, J. Hennig, J. Hennig, S. Glöggler, NMR Biomed. https://doi.org/10.1002/nbm.4400.
[43] G. Stevanato, S. Singha Roy, J. Hill-Cousins, I. Kuprov, L. J. Brown, R. C. D. Brown, G. Pileio, M. H. Levitt, *Phys. Chem. Chem. Phys.* **2015**, *17*, 5913–5922.
[44] K. F. Sheberstov, H. Vieth, H. Zimmermann, B. A. Rodin, K. L. Ivanov, A. S. Kiryutin, A. V. Yurkovskaya, *Sci. Rep.* **2019**, *9*, 20161.
[45] K. F. Sheberstov, H.-M. Vieth, H. Zimmermann, K. L. Ivanov, A. S. Kiryutin, A. V. Yurkovskaya, *Appl. Magn. Reson.* **2018**, *49*, 293–307.
[46] S. J. DeVience, R. L. Walsworth, M. S. Rosen, *Phys. Rev. Lett.* **2013**, *111*, 173002.
[47] N. B. Shustova, T.-C. Ong, A. F. Cozzolino, V. K. Michaelis, R. G. Griffin, M. Dincă, *J. Am. Chem. Soc.* **2012**, *134*, 15061–15070.
[48] Y. Cai, L. Du, K. Samedov, X. Gu, F. Qi, H. H. Y. Sung, B. O. Patrick, Z. Yan, X. Jiang, H. Zhang, J. W. Y. Lam, I. D. Williams, D. L. Phillips, A. Qin, B. Tang, *Chem. Sci.* **2018**, *9*, 4662–4670.
[49] a) T. Hatakeyama, S. Hashimoto, S. Seki, M. Nakamura, *J. Am. Chem. Soc.* **2011**, *133*, 18614–18617; b) D.-C. Huang, C.-H. Kuo, M.-T. Ho, B.-C. Lin, W.-T. Peng, I. Chao, C.-P. Hsu, Y.-T. Tao, *J. Mater. Chem. C* **2017**, *5*, 7935–7943; c) Y. Ueda, H. Tsuji, H. Tanaka, E. Nakamura, *Chem. Asian J.* **2014**, *9*, 1623–1628; d) S. Hashimoto, T. Ikuta, K. Shiren, S. Nakatsuka, J. Ni, M. Nakamura, T. Hatakeyama, *Chem. Mater.* **2014**, *26*, 6265–6271.

[50] J. Mei, N. L. C. Leung, R. T. K. Kwok, J. W. Y. Lam, B. Z. Tang, *Chem. Rev.* **2015**, *115*, 11718–11940.
[51] M. P. Aldred, C. Li, M.-Q. Zhu, *Chem. Eur. J.* **2012**, *18*, 16037–16045.
[52] J. Mei, Y. Hong, J. W. Y. Lam, A. Qin, Y. Tang, B. Z. Tang, *Adv. Mater.* **2014**, *26*, 5429–5479.
[53] Z. He, C. Ke, B. Z. Tang, *ACS Omega* **2018**, *3*, 3267–3277.
[54] M. J. Albers, R. Bok, A. P. Chen, C. H. Cunningham, M. L. Zierhut, V. Y. Zhang, S. J. Kohler, J. Tropp, R. E. Hurd, Y.-F. Yen, S. J. Nelson, D. B. Vigneron, J. Kurhanewicz, *Cancer Res.* **2008**, *68*, 8607–8615.
[55] T. B. Rodrigues, E. M. Serrao, B. W. C. Kennedy, D.-E. Hu, M. I. Kettunen, K. M. Brindle, *Nat. Med.* **2014**, *20*, 93–97.
[56] C. Cabella, M. Karlsson, C. Canapè, G. Catanzaro, S. C. Serra, L. Miragoli, L. Poggi, F. Uggeri, L. Venturi, P. R. Jensen, M. H. Lerche, F. Tedoldi, *J. Magn. Reson.* **2013**, *232*, 45–52.
[57] P. R. Jensen, M. Karlsson, S. Meier, J. Ø. Duus, M. H. Lerche, *Chemistry* **2009**, *15*, 10010–10012.
[58] W. Jiang, L. Lumata, W. Chen, S. Zhang, Z. Kovacs, A. D. Sherry, C. Khemtong, *Sci. Rep.* **2015**, *5*, 9104.
[59] M. H. Lerche, S. Meier, P. R. Jensen, S.-O. Hustvedt, M. Karlsson, J. Ø. Duus, J. H. Ardenkjær-Larsen, *NMR Biomed.* **2011**, *24*, 96–103.

Manuscript received: November 19, 2021
Accepted manuscript online: December 2, 2021
Version of record online: January 5, 2022